

Pseudoscalar Higgs Bosons at the LHC: Production and Decays into Electroweak Gauge Bosons Revisited

Werner Bernreuther¹, Patrick González², Martin Wiebusch³

Institut für Theoretische Physik, RWTH Aachen University, 52056 Aachen, Germany

Abstract

We analyze and compute, within a number of standard model (SM) extensions, the cross sections $\sigma_{A \rightarrow VV'}$ for the production of a heavy neutral pseudoscalar Higgs boson/spin-zero resonance at the LHC and its subsequent decays into electroweak gauge bosons. For comparison we calculate also the corresponding cross sections for a heavy scalar. The SM extensions we consider include a type-II two-Higgs doublet model (2HDM), a 2HDM with 4 chiral fermion generations, the minimal supersymmetric extension of the SM (MSSM), and top-color assisted technicolour models. Presently available phenomenological constraints on the parameters of these models are taken into account. We find that, with the exception of the MSSM, these models permit the LHC cross sections $\sigma_{A \rightarrow VV'}$ to be of observable size. That is, a pseudoscalar resonance may be observable, if it exists, at the LHC in its decays into electroweak gauge bosons, in particular in WW and $\gamma\gamma$ final states.

PACS number(s): 12.60.-i, 12.60.Fr, 12.60Jv, 12.60.Nz, 14.80.Cp

Keywords: Higgs boson decay, weak gauge bosons, standard model extensions

¹Email: breuther@physik.rwth-aachen.de

²Email: gonzalez@physik.rwth-aachen.de

³Email: mwiebusch@physik.rwth-aachen.de

1 Introduction

The search for Higgs bosons or, more general, (spin-zero) resonances is among the major physics goals of present-day collider physics, as the existence of such resonances and the exploration of their properties (production and decay modes, quantum numbers) would yield decisive clues for unraveling the mechanism of electroweak gauge symmetry breaking (EWSB). There is an exhaustive phenomenology of the production and decay modes of the standard model (SM) Higgs boson; likewise, there are extensive theoretical studies of these issues for spin-zero (Higgs) particles predicted by popular SM extensions. (For reviews see, e.g., [1] and [2–6], respectively.)

For the SM Higgs boson H with a mass $m_H \gtrsim 130$ GeV, signatures from the decay modes⁴ $H \rightarrow WW^{(*)}/ZZ^{(*)}$ have the highest discovery potential for this particle at the Tevatron [8] and at the Large Hadron Collider (LHC) [9, 10]. Concerning non-standard neutral Higgs particles it is, in view of unknown model parameters, less clear as to which decay channel is, for a specific production mode, the most promising one. However, the decays $A \rightarrow WW/ZZ$ of a pseudoscalar Higgs boson A are expected to be strongly suppressed. This is because the couplings AVV ($V = W, Z$) must be loop-induced, and they turn out to be very small in two-Higgs doublet extensions (in large parts of their parameter spaces) and in the minimal supersymmetric extension (MSSM) of the SM [11, 12]. In view of this conventional wisdom one might be inclined to conclude that the discovery of a spin-zero resonance in WW and/or ZZ boson events would immediately suggest that it is a scalar, i.e., a $J^{PC} = 0^{++}$ state. We hasten to add that many suggestions and phenomenological studies have been made how the spin and the CP parity of a resonance can actually be measured for these decay modes, irrespective of any theoretical prejudice [3, 13–21].

In this paper we address the question whether there are realistic scenarios which predict the LHC reactions $pp \rightarrow A \rightarrow W^+W^-, ZZ$ to be of observable size. In fact, we analyze a more general class of reactions, namely the production of a pseudoscalar state A and its decay into electroweak gauge bosons, $pp \rightarrow A \rightarrow VV'$, where $VV' \in \{ZZ, WW, \gamma\gamma, Z\gamma\}$. For comparison we also determine the cross sections $pp \rightarrow H \rightarrow VV'$ of a scalar H with mass $m_H \simeq m_A$. We investigate these cross sections within several models that contain a CP-odd and two CP-even spin-zero states, namely the MSSM, a type II two-Higgs doublet model (2HDM) and its extension by a fourth generation of chiral fermions. We briefly address also its extension by heavy vector-like quarks. Due to the non-decoupling nature of Higgs-fermion couplings, the existence of new heavy fermions can enhance both the production cross sections of Higgs bosons and the branching ratios of their decays to VV' . We also discuss top-colour assisted technicolour (TC2) as a paradigm for scenarios with a relatively light composite pseudoscalar boson. Within each of these models we determine the largest possible signal cross sections for $pp \rightarrow A \rightarrow VV'$ by scanning over the experimentally allowed region of the respective parameter space. We

⁴State-of-the-art predictions for $H \rightarrow WW/ZZ \rightarrow 4$ fermions were made in [7].

take into account the constraints that result from the hadronic branching ratio R_b of $Z \rightarrow b\bar{b}$, from flavour observables, from electroweak precision measurements, from direct Higgs-boson searches at the Tevatron, and from theoretical principles/assumptions.

For all models discussed below we assume that the dynamics of the EWSB sector is such that the electrically neutral Higgs resonances are CP eigenstates in the mass basis, at least to very good approximation. It is well known that Higgs-sector CP violation leads to neutral spin-zero mass eigenstates that are, in general, a mixture of a CP-odd and a CP-even component, the latter of which has couplings to WW/ZZ already at tree-level.

In Section 2 we outline the approximations that we used in computing the cross sections $\sigma(pp \rightarrow A, H \rightarrow VV')$, the parameter-space scanning method, the phenomenological constraints, and we list the tools used in this analysis. Section 3 contains our results for the maximal allowed cross sections $\sigma_{A \rightarrow VV'}$ and $\sigma_{H \rightarrow VV'}$ within a type-II 2HDM with Yukawa couplings widely used in the literature. In Section 4 we extend this analysis to a 2HDM with a sequential fourth fermion generation. We comment also on results within a 2HDM extended by heavy vector-like quarks. In Section 5 we compute the maximum allowed cross sections $\sigma_{A \rightarrow VV'}$ within the so-called phenomenological MSSM (pMSSM) [22], and in Section 6 the analogous calculations are performed for a composite pseudoscalar and a scalar spin-zero resonance within TC2. Section 7 contains a summary and our conclusions.

2 Approximations and Scanning Method

Here we make some general remarks on our approximations used for the computation of the signal cross sections and the method we applied for the scans of the respective parameter spaces of the models below. These models contain two CP-even spin-zero states h and H (by convention the heavier one is denoted by H , except in the TC2 models in Sect. 6) and a CP-odd state A . Since we are mainly interested in the production of A and its decays into massive gauge bosons, we focus on pseudoscalars with $m_A \gtrsim 200$ GeV. If the mass of A is significantly above the top-quark pair production threshold then $A \rightarrow t\bar{t}$ is the dominant decay mode in significant portions of the parameter spaces of these models. In view of our aim of investigating whether or not the processes $pp \rightarrow A \rightarrow VV'$ are relevant for the LHC, we therefore consider, in the above non-SUSY models, a pseudoscalar with $m_A \lesssim 2m_t$. Likewise, the investigation of $pp \rightarrow H \rightarrow VV'$, made mainly for the purpose of comparison with the pseudoscalar cross sections, is confined to scalars H with $m_H \lesssim 2m_t$. Furthermore, we compute also the total Tevatron production cross section for the light Higgs boson h (whose mass is arbitrary in the non-SUSY models below) and compare with experimental exclusion limits.

In each model we will use the narrow-width approximation in computing the cross sections for the production of $\phi = A, H, h$ and its subsequent decay into $VV' =$

$WW, ZZ, Z\gamma, \gamma\gamma$. To ensure the validity of this approximation, we constrain model parameters such that the total width to mass ratio Γ_ϕ/m_ϕ is always less than 0.2.

The dominant Higgs-boson production mechanism at the LHC is gluon fusion. For all models discussed below, the corresponding partonic cross sections $\sigma(gg \rightarrow \phi)_{\text{BSM}}$ are calculated in the effective coupling approximation [23]. In this approximation the cross section $\sigma(gg \rightarrow \phi)_{\text{BSM}}$ in an SM extension is obtained by rescaling the SM cross section by the ratio of $\phi \rightarrow gg$ decay widths:

$$\sigma(gg \rightarrow \phi)_{\text{BSM}} \approx \sigma(gg \rightarrow H_{\text{ref}})_{\text{SM}} \frac{\Gamma(\phi \rightarrow gg)_{\text{BSM}}}{\Gamma(H_{\text{ref}} \rightarrow gg)_{\text{SM}}} \quad , \quad (1a)$$

where H_{ref} is a Higgs boson with $m_{H_{\text{ref}}} = m_\phi$ and SM couplings. In some models, for instance the 2HDM or the MSSM at large $\tan\beta$, the $b\bar{b}$ production mode becomes important, too [24–26]. In these cases we approximate the $b\bar{b} \rightarrow \phi$ cross section analogously by

$$\sigma(b\bar{b} \rightarrow \phi)_{\text{BSM}} \approx \sigma(b\bar{b} \rightarrow H_{\text{ref}})_{\text{SM}} \frac{\Gamma(\phi \rightarrow b\bar{b})_{\text{BSM}}}{\Gamma(H_{\text{ref}} \rightarrow b\bar{b})_{\text{SM}}} \quad . \quad (1b)$$

The SM production cross sections and decay widths were calculated with **FeynHiggs** [27]. For the production cross sections⁵ **FeynHiggs** includes NNLO QCD corrections and NNLL soft gluon resummation effects by interpolating the tables from [29]. The cross sections given below refer to the LHC at $\sqrt{s} = 14 \text{ TeV}$.

We have scanned the parameter space of each model, choosing parameter sets randomly and discarding them if they violate theoretical or experimental bounds. The theoretical bounds we considered include vacuum stability, perturbativity and tree level unitarity. On the experimental side we implemented constraints from direct Higgs boson searches at LEP2 and Tevatron by using **HiggsBounds** [30], fits of the oblique electroweak parameters S , T , and U [31, 32] and flavour observables measured in B - \bar{B} mixing and $b \rightarrow s\gamma$ decays. More information on these bounds and their implementation in our analysis is given below in the discussions of the individual models. We used an adaptive sampling technique along the lines of [33] in order to find those regions within the allowed parameter space of each model where the signal cross sections are large.

Throughout this paper we will use the following SM parameters:

$$\begin{aligned} 1/\alpha_{\text{em}} &= 137.036 \quad , \quad \alpha_s = 0.118 \quad , \\ m_Z &= 91.19 \text{ GeV} \quad , \quad m_W = 80.40 \text{ GeV} \quad , \\ m_t &= 172.6 \text{ GeV} \quad , \quad m_b = 4.79 \text{ GeV} \quad , \quad m_\tau = 1.78 \text{ GeV} \quad , \quad V_{tb} = 1 \quad . \end{aligned} \quad (2)$$

As to the 2HDM extensions discussed in this paper, we use conventional type-II Yukawa interactions (cf. the comment at the end of Section 3); i.e. the Yukawa couplings of the quarks and leptons of the first and second generation are assumed to be small. Therefore, their interactions with the Higgs resonances will be neglected in the analysis below. For the calculation of the decay widths at one-loop we used **FeynArts** 3.4 [34, 35] in combination with **FormCalc** 6.0 and **LoopTools** 2.3 [36, 37].

⁵See [28] for an overview of the NNLO QCD computations of $\sigma(p\bar{p}, pp \rightarrow \phi + X)$.

3 Type-II Two-Higgs Doublet Model

A simple class of SM extensions which contain a pseudoscalar Higgs particle are the two Higgs doublet models (2HDM), where a second complex Higgs doublet is added to the SM. Extensive literature exists on these models and their phenomenological implications [38]. For the convenience of the reader, and in order to fix our notation, we provide here a brief summary of the model parameters and the physical particle content.

Following the conventions of [39], we denote the two complex scalar doublets as $\Phi_1 = (\phi_1^+, \phi_1^0)^\top$ and $\Phi_2 = (\phi_2^+, \phi_2^0)^\top$. The most general $SU(2) \times U(1)$ invariant tree-level Higgs potential can then be written as

$$\begin{aligned} V = & m_{11}^2 \Phi_1^\dagger \Phi_1 + m_{22}^2 \Phi_2^\dagger \Phi_2 - [m_{12}^2 \Phi_1^\dagger \Phi_2 + \text{h.c.}] \\ & + \frac{1}{2} \lambda_1 (\Phi_1^\dagger \Phi_1)^2 + \frac{1}{2} \lambda_2 (\Phi_2^\dagger \Phi_2)^2 + \lambda_3 (\Phi_1^\dagger \Phi_1) (\Phi_2^\dagger \Phi_2) + \lambda_4 (\Phi_1^\dagger \Phi_2) (\Phi_2^\dagger \Phi_1) \\ & + \left[\frac{1}{2} \lambda_5 (\Phi_1^\dagger \Phi_2)^2 + (\lambda_6 \Phi_1^\dagger \Phi_1 + \lambda_7 \Phi_2^\dagger \Phi_2) (\Phi_1^\dagger \Phi_2) + \text{h.c.} \right] \quad . \end{aligned} \quad (3)$$

There are strong constraints on λ_6 and λ_7 , since these are coefficients of terms which give rise to flavour-changing neutral currents. We therefore set $\lambda_6 = \lambda_7 = 0$. To ensure CP conservation in the Higgs sector at tree level we require the remaining parameters to be real without loss of generality. If these parameters are chosen in such a way that the electric charge is conserved, we can write the vacuum expectation values (VEVs) of the Higgs doublets as

$$\langle \Phi_1 \rangle = \frac{1}{\sqrt{2}} \begin{pmatrix} 0 \\ v_1 \end{pmatrix} \quad , \quad \langle \Phi_2 \rangle = \frac{1}{\sqrt{2}} \begin{pmatrix} 0 \\ v_2 \end{pmatrix} \quad , \quad (4)$$

with $v_1, v_2 \in \mathbb{R}$, and $v_1^2 + v_2^2 = v^2 \approx (246 \text{ GeV})^2$ in order to obtain the correct W and Z boson masses. After expanding the fields around their VEVs and diagonalising the mass matrices, the real components of the Higgs doublets mix and yield two neutral scalar mass eigenstates:

$$H = (\sqrt{2} \text{Re } \phi_1^0 - v_1) \cos \alpha + (\sqrt{2} \text{Re } \phi_2^0 - v_2) \sin \alpha \quad , \quad (5a)$$

$$h = -(\sqrt{2} \text{Re } \phi_1^0 - v_1) \sin \alpha + (\sqrt{2} \text{Re } \phi_2^0 - v_2) \cos \alpha \quad . \quad (5b)$$

By convention, h denotes the lighter of the two states. In addition, the physical particle spectrum contains one neutral pseudoscalar state A and a charged Higgs boson and its conjugate, H^\pm . Expressions for the mixing angle α , v_1 , v_2 and the mass eigenvalues m_h , m_H , m_A , and m_{H^\pm} in terms of the parameters of the Higgs potential can be found in [39]. Using these expressions, we can describe the 2HDM parameter space by the following set of independent parameters:

$$\tan \beta \equiv v_2/v_1 \quad , \quad \beta - \alpha \quad , \quad m_h \quad , \quad m_H \quad , \quad m_A \quad , \quad m_{H^\pm} \quad , \quad \lambda_1 \quad . \quad (6)$$

As already mentioned above, the Yukawa sector we use here is that of a type-II model, i.e., the doublet Φ_2 couples only to up-type fermions and Φ_1 only to down-type fermions.

Experimental bounds on this type of 2HDMs have been discussed in several papers, including [40–43]. More recently a comprehensive study of the allowed parameter space of the (CP -violating) type II 2HDM was performed [44], which combined several theoretical and experimental constraints. The theoretical constraints considered in that work are positivity of the Higgs potential, tree-level unitarity of the S matrix [45], and perturbativity. On the experimental side the relevant bounds come from direct Higgs-boson searches at LEP2 and the Tevatron, LEP measurements [46] of the oblique electroweak parameters⁶ S , T and U and of the ratio $R_b = \Gamma(Z \rightarrow b\bar{b})/\Gamma(Z \rightarrow \text{hadrons})$. There are also several constraints on the 2HDM parameter space from flavour physics. The strongest ones come from observables measured in B - \bar{B} mixing and $B \rightarrow X_s \gamma$ decays [44]. The bounds from R_b , B - \bar{B} mixing, and $B \rightarrow X_s \gamma$ decays only constrain the parameters $\tan \beta$ and m_{H^\pm} and become relevant for $m_{H^\pm} \lesssim 300 \text{ GeV}$ or $\tan \beta \lesssim 1$. However, their combination with bounds from the oblique electroweak parameters can still constrain the neutral Higgs boson sector, because the states H^\pm with a mass that is very different from the neutral Higgs-boson masses leads to large contributions to T . Combining the constraints from R_b and the oblique electroweak parameters, we obtain the lower bound

$$\tan \beta \gtrsim 0.7 \tag{7}$$

on this parameter.

Our scans of the parameter space of the 2HDM, which lead in particular to the bound (7), were made as described in Section 2. The experimental and theoretical constraints were implemented by interfacing with several publicly available codes. Positivity, tree-level unitarity and perturbativity were checked with **2HDMC 1.0.6** [49]. The perturbativity bound was implemented by requiring that the dimensionless couplings from the Higgs potential satisfy $|\lambda_1|, \dots, |\lambda_5| < 4\pi$. The bounds from direct Higgs-boson searches at LEP2 and the Tevatron were checked with **HiggsBounds 1.2.0** [30], which provides a model-independent method for deciding whether or not a specific parameter is excluded at 95% C.L. The oblique electroweak parameters were calculated with **FeynArts 3.4**, **FormCalc 6.0**, and **LoopTools 2.3**. The numerical results were compared with those computed by **2HDMC** and perfect agreement was found. In the relevant parameter space region of the 2HDM the contribution to U is too small to lead to any constraints. The best-fit values of S and T , their standard deviations and correlation coefficient were taken from [50, 51]. In our scan we discarded model parameters that lie outside the 95% C.L. ellipse in the S - T -plane. Model parameters that violate the R_b bound at 95% C.L. were discarded by using the respective equations from [41]. Finally, the flavour physics bounds are obeyed by requiring $m_{H^\pm} > 360 \text{ GeV}$.

With these constraints we have computed the cross sections $\sigma_{A \rightarrow VV'}$, $\sigma_{H \rightarrow VV'}$ for the LHC reactions $pp \rightarrow A \rightarrow VV'$ and $pp \rightarrow H \rightarrow VV'$ using the approximations described in Section 2. Figure 1 shows scatter plots of the combinations of $\sigma(pp \rightarrow H \rightarrow VV')$ and $\sigma(pp \rightarrow A \rightarrow VV')$ (with $VV' = WW, ZZ, \gamma\gamma, Z\gamma$) that we found within the

⁶In [47, 48] formulae were given for these parameters for multi-Higgs extensions of the SM.

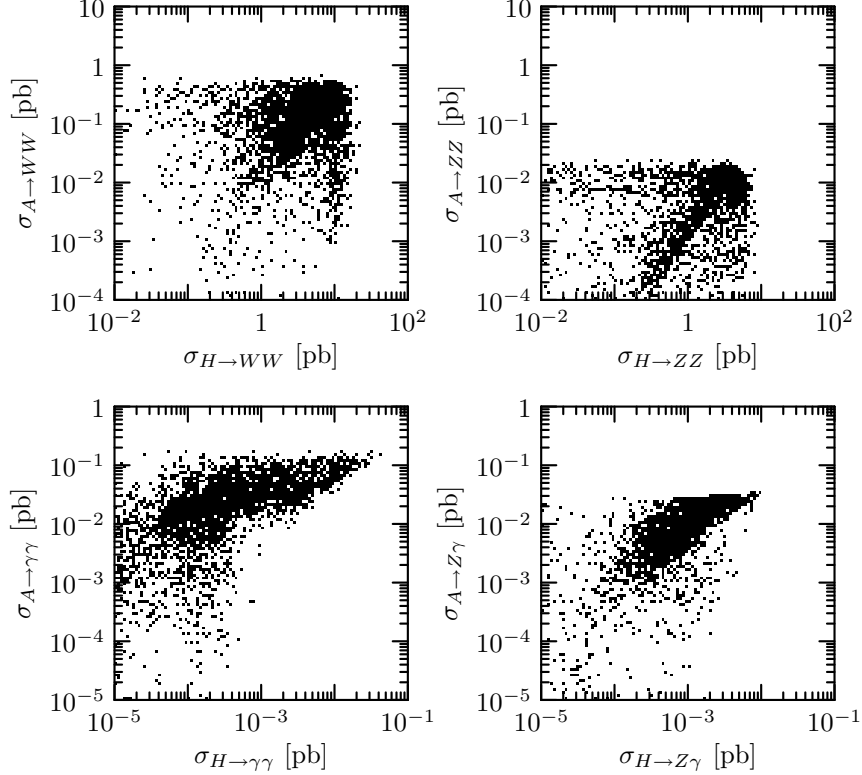


Figure 1: Scatter plots of the LHC cross sections $\sigma_{H \rightarrow VV'}$ versus $\sigma_{A \rightarrow VV'}$ in the 2HDM.

allowed parameter space. Separate parameter scans were performed for each final state. The importance function (in the sense of [33]) was set to $\sigma(pp \rightarrow A \rightarrow VV')$ if the parameter set passes the constraints discussed above and to zero otherwise. This means that the scanning algorithm seeks out those regions of the allowed parameter space where σ_A is large. The density of the points in Fig. 1 does therefore *not* represent a probability density under the assumption of a flat prior. It does, however, give a qualitative measure of the amount of fine tuning required to obtain certain combinations of cross sections. The figures show that for the $\gamma\gamma$ and $Z\gamma$ final states a large cross section σ_H is typically accompanied by a large σ_A . For the WW and ZZ final states there is no strong correlation. We find that the maximum values of the cross sections $\sigma_{A \rightarrow VV'}$ are

$$\begin{aligned} \sigma(pp \rightarrow A \rightarrow WW) &\lesssim 0.7 \text{ pb} \quad , & \sigma(pp \rightarrow A \rightarrow ZZ) &\lesssim 0.03 \text{ pb} \quad , \\ \sigma(pp \rightarrow A \rightarrow \gamma\gamma) &\lesssim 0.2 \text{ pb} \quad , & \sigma(pp \rightarrow A \rightarrow Z\gamma) &\lesssim 0.04 \text{ pb} \quad . \end{aligned} \quad (8)$$

There are two scenarios in which the cross sections $\sigma_{A \rightarrow VV'}$ become maximal simultaneously:

$$\begin{aligned} \tan \beta &\approx 0.75 \quad , \quad m_A = 320 \text{ GeV} \quad , \quad m_{H^\pm} > 370 \text{ GeV} \quad , \\ \beta - \alpha &\approx \frac{\pi}{2} \quad \text{or} \quad m_h > m_A - m_Z \quad , \end{aligned} \quad (9)$$

where the values in the first line hold for both scenarios. The cross sections σ_A are most sensitive to $\tan\beta$ and m_A . It is well known that small values of $\tan\beta$ lead to larger production rates for pseudoscalar Higgs bosons, because the main Higgs production mechanism at the LHC is $gg \rightarrow \phi$ mediated by a top-quark loop with the $At\bar{t}$ coupling being proportional to $\cot\beta$. At the same time the $A \rightarrow VV'$ partial widths are enhanced, because they are dominated by top-quark loops. The above lower bound on m_{H^\pm} is then necessary for avoiding the R_b bound. If the mass of the pseudoscalar A is sufficiently large but below the $t\bar{t}$ threshold then there is no phase-space suppression of the decays into massive gauge bosons while the competing decay channel $A \rightarrow t\bar{t}$ is closed. As $A \rightarrow b\bar{b}$ has a small rate for $\tan\beta \sim 1$, the $A \rightarrow Zh$ decay would be the dominant one in this case. However, this decay can be parametrically or kinematically suppressed, which then further increases the $A \rightarrow VV'$ branching ratios. This corresponds to the two options in (9). Kinematical suppression takes place if the light Higgs boson h is sufficiently heavy while parametric suppression happens if $\beta - \alpha \approx \pi/2$. This takes us close to the so-called decoupling limit, which is defined by $m_H, m_A, m_{H^\pm} \gg m_h$ and $\cos(\beta - \alpha) \ll 1$ [39]. In this limit the couplings of h to the weak gauge bosons are SM-like, while the (tree-level) couplings of the heavy Higgs boson H to WW and ZZ and thus $H \rightarrow WW, ZZ$ are suppressed. Moreover, the $A \rightarrow Zh$ partial width is suppressed by a factor of $\cos^2(\beta - \alpha)$. However, the $pp \rightarrow H \rightarrow WW, ZZ$ cross sections can still be of the order of 10 pb in this scenario, if $\beta - \alpha$ is only slightly different from $\pi/2$.

In a second series of scans we took the cross sections $\sigma_{H \rightarrow VV'}$ to be the respective importance function and found the following upper limits:

$$\begin{aligned} \sigma(pp \rightarrow H \rightarrow WW) &\lesssim 26 \text{ pb} \quad , & \sigma(pp \rightarrow H \rightarrow ZZ) &\lesssim 10 \text{ pb} \quad , \\ \sigma(pp \rightarrow H \rightarrow \gamma\gamma) &\lesssim 0.016 \text{ pb} \quad , & \sigma(pp \rightarrow H \rightarrow Z\gamma) &\lesssim 0.1 \text{ pb} \quad . \end{aligned} \quad (10)$$

Here the maximal values are also reached for $\tan\beta \approx 0.75$, because the $Ht\bar{t}$ coupling is proportional to $1/\sin\beta$; i.e., small $\tan\beta$ increases the $gg \rightarrow H$ production cross section. Accordingly, the R_b bound requires the H^\pm to be sufficiently heavy. Furthermore, h should be heavy enough so that $H \rightarrow hh$ decays are kinematically forbidden. However, unlike the above cross sections for A , the cross sections (10) do not reach their maximal values in the same region of parameter space. The cross section for the $\gamma\gamma$ final state is maximal for parameters similar to those in (9):

$$\begin{aligned} \tan\beta &\approx 0.75 \quad , & m_H &= 265 \text{ GeV} \quad , & m_{H^\pm} &> 370 \text{ GeV} \quad , \\ \beta - \alpha &\approx \frac{\pi}{2} \quad , & m_h &> m_H/2 \quad . \end{aligned} \quad (11)$$

These values of $\beta - \alpha$ suppress the $H \rightarrow WW, ZZ$ decays, which would otherwise give large contributions to the total H width. Of course, the cross sections for the WW and ZZ final states are maximal in a region where these decays are not suppressed:

$$\begin{aligned} \tan\beta &\approx 0.75 \quad , & m_H &= 220 \text{ GeV} \quad , & m_{H^\pm} &> 370 \text{ GeV} \quad , \\ \alpha &\approx \frac{\pi}{2} \quad , & m_h &> m_H/2 \quad . \end{aligned} \quad (12)$$

The cross section for the $Z\gamma$ final state reaches its maximum in a very different region of parameter space, namely where the $H \rightarrow WW, ZZ$ decays are kinematically forbidden and the dominant contribution to the $H \rightarrow Z\gamma$ decay width comes from bosonic loops:

$$\begin{aligned} \tan \beta &\approx 0.9 \quad , \quad m_h = m_H = 150 \text{ GeV} \quad , \\ m_A, m_{H^\pm} &> 315 \text{ GeV} \quad , \quad \alpha \approx \frac{\pi}{2} \quad . \end{aligned} \tag{13}$$

The type II 2HDM we considered here is a popular subject of investigations due to its close relation to the Higgs sector of the minimal supersymmetric SM. It is, however, by no means the only possible choice for a 2HDM Yukawa sector. Extending the present analysis to a wider range of 2HDM models could be a subject for future studies. An interesting variant of a 2HDM, based on the requirement of maximal CP invariance, was proposed in [52], and its LHC phenomenology was investigated in [53]. This model contains an SM-like scalar h_1 , while the two other physical neutral Higgs boson states h_2 and h_3 have unusual Yukawa couplings. Moreover, both h_2 and h_3 do not have tree-level couplings to WW and ZZ .

4 A Heavy Fourth Generation

Recently, there has been renewed interest in the phenomenology of the SM extended by a sequential fourth generation of heavy chiral quarks and leptons (SM4). It was found [54–56] that such fermions with masses in the (few) hundred GeV range can exist, in spite of strong experimental constraints. The presence of a heavy fourth generation would certainly affect the cross sections for Higgs-boson production at the Tevatron and the LHC, because the dominant production mode, $gg \rightarrow \phi$, would receive additional contributions from loops of the fourth generation quarks. Additionally, the partial widths of the loop-mediated $\phi \rightarrow VV'$ decays would be affected. Since, in this paper, we are mainly interested in pseudoscalar Higgs bosons, we will now study the extension of the type II 2HDM from the last section by a fourth generation of chiral fermions (2HDM4). We denote the additional fermions by u_4, d_4, ℓ_4 and ν_4 and assume ν_4 to be a Dirac particle. For simplicity we also assume that the mixing between the fourth and the first three generations is strongly suppressed. It is, however, worth noting that studies [57, 58] of the SM plus a fourth generation with a general unitary 4×4 CKM matrix showed that large mixing between the fourth and the first three generations is still allowed experimentally.

The strongest constraints on the masses of the additional fermions come from direct searches at LEP2 and at the Tevatron, and from electroweak precision observables. Non-observation at LEP2 implies the lower bounds $m_{\ell_4, \nu_4} \gtrsim 100 \text{ GeV}$. Searches for heavy quarks at the Tevatron lead to the bounds $m_{u_4} > 311 \text{ GeV}$ [59] and $m_{d_4} > 338 \text{ GeV}$ [60]. Experimental bounds on the S, T , and U parameters additionally constrain the mass

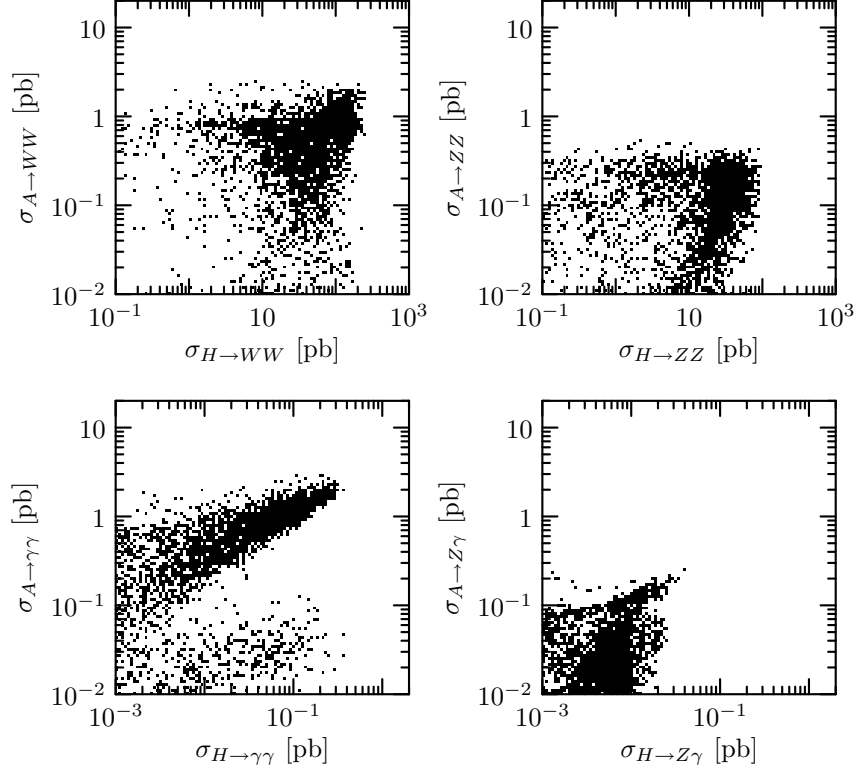


Figure 2: Scatter plots of the LHC cross sections $\sigma_{H \rightarrow VV'}$ versus $\sigma_{A \rightarrow VV'}$ in the 2HDM4.

splittings within the $SU(2)$ doublets. Large mass splittings of the $I_W = \pm 1/2$ partners of a doublet yield large corrections to the T parameter, while small mass splittings result in large contributions to the parameter S .

For our parameter scans we used the same bounds and tools as for the 2HDM in Section 3. We modified our calculations of the S , T , and U parameters and included the contributions from the extended Higgs sector and the fourth generation fermions. The latter contributions were compared to the results from [54] and perfect agreement was found. To ensure perturbativity of the Yukawa sector we required that the Yukawa couplings of the new fermions lie between -4π and $+4\pi$. Finally, the above-mentioned lower bounds on the masses of the fourth generation fermions were used:

$$m_{\ell_4, \nu_4} > 100 \text{ GeV} \quad , \quad m_{u_4} > 311 \text{ GeV} \quad , \quad m_{d_4} > 338 \text{ GeV} \quad . \quad (14)$$

Figure 2 shows scatter plots of the resulting cross sections $\sigma_{H \rightarrow VV'}$ and $\sigma_{A \rightarrow VV'}$ for the various final states. The maximum allowed values of the cross sections for A are:

$$\begin{aligned} \sigma(pp \rightarrow A \rightarrow WW) &\lesssim 3.2 \text{ pb} \quad , & \sigma(pp \rightarrow A \rightarrow ZZ) &\lesssim 0.40 \text{ pb} \quad , \\ \sigma(pp \rightarrow A \rightarrow \gamma\gamma) &\lesssim 3.0 \text{ pb} \quad , & \sigma(pp \rightarrow A \rightarrow Z\gamma) &\lesssim 0.26 \text{ pb} \quad . \end{aligned} \quad (15)$$

They are about one order of magnitude larger than the corresponding bounds in the

three-generation 2HDM. All the cross sections reach their maximal values in the following region of parameter space:

$$\begin{aligned} \tan \beta \approx 6.3 \quad , \quad m_A \approx 260 \text{ GeV} \quad , \quad m_{H\pm} \approx 360 \text{ GeV} \quad , \quad \alpha \approx \beta - \frac{\pi}{2} \quad , \\ m_{\nu_4} \approx 100 \text{ GeV} \quad , \quad m_{\ell_4} \approx m_A/2 \quad . \end{aligned} \quad (16)$$

The cross sections $\sigma_{A \rightarrow VV'}$ have only a weak dependence on the model parameters that are not stated in (16). Of course, these parameters are subject to the experimental and theoretical constraints of Section 2. Interestingly, a degenerate fourth generation quark doublet is still allowed in the 2HDM4, even though it would be excluded in the SM4. The reason is that the large contribution to S from the degenerate quark doublet combined with the large contribution to T from the extended Higgs sector pushes the model back into the 95% C.L. ellipse in the S - T -plane. For the parameters above and $m_{u_4} = m_{d_4} \simeq 330 \text{ GeV}$ the shifts in S and T with respect to the SM, with a Higgs-boson whose mass is 117 GeV , are

$$\Delta S = 0.22 \quad , \quad \Delta T = 0.20 \quad . \quad (17)$$

The main reason for the large cross sections $\sigma_{A \rightarrow VV'}$ in this model is a dramatic increase of the pseudoscalar production rate $\sigma(gg \rightarrow A)$, as compared to the 2HDM with three generations. This increase is due to additional contributions from loops of the fourth generation quarks. The couplings of A to up-type (down-type) quarks are proportional to $\cot \beta$ ($\tan \beta$). As we use conventional type-II Yukawa interactions both types of couplings are proportional to the respective fermion mass. Since the 2HDM4 contains a heavy down-type quark d_4 , the $Ad_4\bar{d}_4$ coupling becomes strong for large values of $\tan \beta$. The value of $\tan \beta$ is bounded from above by the perturbativity constraint on the Yukawa couplings of the fourth generation fermions, which yields $\tan \beta \lesssim 6.3$. The constraints from R_b and $b \rightarrow s\gamma$ impose a lower bound on $\tan \beta$ and thus on the strength of the $Au_4\bar{u}_4$ coupling, but it is the maximally allowed value $\tan \beta \approx 6.3$ that leads to the bounds (15). For this value of $\tan \beta$ the gluon-fusion induced LHC cross section $\sigma(gg \rightarrow A)$ can become as large as $\sim 840 \text{ pb}$ in the 2HDM4. The resulting huge pseudoscalar Higgs-boson production rate would of course dramatically increase the likelihood for A being discovered in other decay modes like $A \rightarrow b\bar{b}$, $A \rightarrow \tau\bar{\tau}$, or perhaps even in $A \rightarrow gg$ dijet events. With the parameters that yield $\sigma(gg \rightarrow A) = 840 \text{ pb}$ we obtain the branching ratios

$$B(A \rightarrow gg) \simeq 0.46 \quad , \quad B(A \rightarrow b\bar{b}) \simeq 0.43 \quad , \quad , B(A \rightarrow \tau^+\tau^-) \simeq 0.05 \quad . \quad (18)$$

The $\tau\tau$ final state allows also for a determination of the CP quantum numbers of the Higgs-boson resonance [61, 62].

If the values of $\beta - \alpha$ and m_A are as in (16) and if m_H is sufficiently large, we are in the decoupling limit [39]. As far as the Yukawa couplings are concerned, for $\tan \beta \sim 6.3$ only the couplings of the heavy Higgs bosons to down-type quarks are enhanced, while

the couplings of the light Higgs boson have similar magnitudes as the SM couplings, but the $hu\bar{u}$ and $hd\bar{d}$ couplings differ by a sign for $\alpha > 0$. The u_4 - and d_4 -loop contributions to the $gg \rightarrow h$ amplitude depend sensitively on α . For α being small and positive there are cancellations. In fact, for $\alpha = \pi/2 - \beta$ and $m_{u_4} = m_{d_4}$ the u_4 - and d_4 -loop would almost exactly cancel, and the h production cross section at the Tevatron would essentially be the same as the SM cross section. Disregarding this extreme fine tuning we consider a set of values α in the vicinity of (16) and m_{u_4}, m_{d_4} such that the gluon-fusion induced Tevatron production cross section $\sigma(gg \rightarrow h)$ is about four times larger than the SM rate. (Without the extended Higgs sector one would expect a factor of 9.) If one takes into account the other production modes that are relevant at the Tevatron, $q\bar{q}' \rightarrow Wh, Zh$, one finds that the total Tevatron h production cross section is larger than the SM cross section by a factor of about 3.5. This does not invalidate this “maximum scenario”. A closer analysis, using **HiggsBounds** [30], yields that for the parameters in (16) that a light Higgs boson h with a mass between 145 GeV and 194 GeV is excluded by the data from direct Tevatron searches. The recently published data [8] will widen this exclusion window, but will not falsify the above scenario.

While pseudoscalar Higgs-boson production via gluon fusion can only be mediated by quark loops, the decays into electroweak gauge bosons can also be mediated by loops of leptons or neutrinos. As the mass bounds from direct searches for fourth generation leptons are still relatively low, it is possible to construct a situation where m_A is close to the $\ell_4\bar{\ell}_4$ threshold. In that case the ℓ_4 -loop contribution to $\Gamma(A \rightarrow VV')$ is kinematically enhanced, which leads to larger branching ratios. However, since fixed order calculations are unreliable at threshold we conservatively require a minimum difference of 10 GeV between m_{ℓ_4} and $m_A/2$. The upper limits (15) for the pseudoscalar cross sections were obtained with this requirement and might actually be slightly bigger. For the $ZZ, \gamma\gamma$ and $Z\gamma$ final states the branching ratios could be further increased by setting $m_{\nu_4} \approx m_A/2$, too. However, it turns out that the constraints on S and T forbid such a choice of parameters.

The upper limits on the cross sections for the heavy scalar Higgs boson are:

$$\begin{aligned} \sigma(pp \rightarrow H \rightarrow WW) &\lesssim 280 \text{ pb} \quad , & \sigma(pp \rightarrow H \rightarrow ZZ) &\lesssim 110 \text{ pb} \quad , \\ \sigma(pp \rightarrow H \rightarrow \gamma\gamma) &\lesssim 0.41 \text{ pb} \quad , & \sigma(pp \rightarrow H \rightarrow Z\gamma) &\lesssim 0.045 \text{ pb} \quad . \end{aligned} \quad (19)$$

The cross sections associated with the loop-induced H decays, $\sigma(pp \rightarrow H \rightarrow \gamma\gamma, Z\gamma)$, become maximal simultaneously with the cross sections $\sigma_{A \rightarrow VV'}$, i.e. for the parameters (16). For the cross sections $\sigma(pp \rightarrow H \rightarrow WW, ZZ)$ the relevant parameters are $\tan\beta$, m_H , $\beta - \alpha$ and m_h . The maximal values are reached for

$$\tan\beta \approx 5.7 \quad , \quad m_H \approx 210 \text{ GeV} \quad , \quad \beta - \alpha \approx \frac{\pi}{4} \quad , \quad m_h > m_H/2 \quad . \quad (20)$$

This can be understood as follows: the couplings of H to up-type quarks are proportional to $\sin\alpha/\sin\beta$ while its couplings to down-type quarks are proportional $\cos\alpha/\cos\beta$. Therefore, for reasons analogous to those discussed for the A production cross sections,

the largest H production rates are obtained for large $\tan\beta$, i.e. for an enhanced $Hd_4\bar{d}_4$ coupling. This coupling is increased further if the mixing angle α is small. However, the (tree-level) partial widths for $H \rightarrow WW, ZZ$ are proportional to $\cos^2(\beta - \alpha)$ and would be suppressed for large $\tan\beta$ and a small α . In the search for the largest cross sections $\sigma(gg \rightarrow H \rightarrow WW, ZZ)$, the best compromise turns out to be the choice $\beta - \alpha = \pi/4$. Within the region of m_H values allowed by direct Higgs-boson searches, the $gg \rightarrow H \rightarrow WW, ZZ$ cross sections steadily increase for decreasing m_H , i.e., the largest cross sections are obtained for relatively small m_H . Finally the mass m_h of the light Higgs boson must be large enough so that the competing $H \rightarrow hh$ decay mode is kinematically forbidden. The masses of the fourth generation fermions have very little influence on the $gg \rightarrow H \rightarrow WW, ZZ$ cross sections in this scenario, as long as they are in agreement with the mass bounds (14) and the constraints on S and T .

A more exotic possibility for new heavy fermions are vector-like quarks, i.e., quarks whose left- and right-chiral components have equal gauge charges (see, e.g. [63–66]). Such states are present in a number of SM extensions, including extra dimensional models with bulk fermions [67] and Little Higgs models [68]. In [69] we presented an extension of the 2HDM by one $SU(2)$ singlet and two doublets of vector-like quarks and computed the loop contributions of these new fermions to the pseudoscalar decay widths. However, if the constraints from the oblique electroweak parameters are applied to this model it turns out that these contributions do not alter the results presented for the three-generation 2HDM in section 3 in any noticeable way.

5 The MSSM

The decays of the scalar Higgs bosons in the MSSM have already been discussed in detail in the literature. (See [2] for a review.) In this section we will therefore concentrate on the cross sections $\sigma(pp \rightarrow A \rightarrow VV')$ for the pseudoscalar Higgs boson A . In [12] the branching ratios of A into gauge bosons were calculated under the assumption that all SUSY particles are too heavy to yield relevant contributions to the effective AVV' couplings. However, experimental bounds on chargino and neutralino masses are still relatively weak and values as low as 100 GeV or 60 GeV, respectively, are still possible.⁷ We have therefore extended the results of [12] to include the contributions of SUSY particles to the loop-mediated $gg \rightarrow A$ production mechanism and the $A \rightarrow VV'$ decays. We will see that these contributions are relevant in those regions of the MSSM parameter space that maximize the $pp \rightarrow A \rightarrow VV'$ cross sections. To avoid misunderstandings: we consider here the MSSM with three generations.

The Higgs sector of the MSSM is that of a type-II 2HDM discussed in section 3, but with a much more restricted parameter space. In the MSSM the masses of the neutral

⁷If the requirement of gauge unification at the GUT scale is dropped, the lightest neutralino could even be massless.

Higgs bosons and the mixing angle α are no longer independent parameters. At tree level they can be expressed in terms of the pseudoscalar Higgs-boson mass m_A and $\tan \beta$ as follows:

$$m_{H^\pm}^2 = m_A^2 - m_W^2 \quad , \quad (21a)$$

$$m_{H,h}^2 = \frac{1}{2} \left[m_A^2 + m_Z^2 \pm \sqrt{(m_A^2 + m_Z^2)^2 - 4m_Z^2 m_A^2 \cos^2 2\beta} \right] \quad , \quad (21b)$$

$$\cos(2\alpha) = -\cos(2\beta) \frac{m_A^2 - m_Z^2}{m_H^2 - m_h^2} \quad , \quad \sin(2\alpha) = -\sin(2\beta) \frac{m_H^2 + m_h^2}{m_H^2 - m_h^2} \quad . \quad (21c)$$

For MSSM scenarios with $m_A \gg m_Z$ these equations yield

$$m_A \approx m_H \quad , \quad \beta - \alpha \approx \frac{\pi}{2} \quad . \quad (22)$$

However, it is well-known that the tree-level relations (21) are substantially modified by loop corrections to the MSSM Higgs potential. These corrections are responsible for pushing the mass of the light Higgs boson substantially above the Z -boson mass and have to be taken into account to obtain reliable results. In our scans we used **FeynHiggs** 2.6.5 [27, 70–72] to calculate all one-loop and leading two-loop corrections to the neutral Higgs-boson self-energies in the MSSM and to extract from them the physical neutral Higgs-boson masses, LSZ residues, and the resulting effective mixing angle α_{eff} . We also use **FeynHiggs** for the calculation of the total Higgs-boson decay widths.

As mentioned above, contributions from SUSY particles have to be taken into account when calculating the amplitudes for the loop-mediated production or decay processes. At the one-loop level, the decay amplitudes of the Higgs bosons receive also contributions from loops of squarks, sleptons, charginos and neutralinos. However, the squark and slepton loop contributions to the pseudoscalar Higgs decays vanish since parity is conserved in the bosonic sector of the MSSM. For the same reason the $gg \rightarrow A$ production amplitude receives no new contributions, while the $gg \rightarrow H$ process is now also mediated by squark loops.

The MSSM contains a large number of parameters due to the soft SUSY-breaking part of the Lagrangian. To make phenomenological studies feasible, the number of free parameters has to be reduced significantly. In this paper we will work in the so-called phenomenological MSSM (pMSSM) [22], where the number of parameters is reduced to 22 by making several phenomenologically motivated assumptions, including the absence of both new CP -violating phases and new sources of flavour violation. The independent parameters of the pMSSM are

- $\tan \beta$ and m_A ,
- the Higgs-Higgsino mass parameter μ ,

- the gaugino mass parameters M_1 , M_2 , and M_3 ,
- the light sfermion mass parameters $m_{\tilde{q}}$, $m_{\tilde{u}_R}$, $m_{\tilde{d}_R}$, $m_{\tilde{l}}$, and $m_{\tilde{e}_R}$,
- the light sfermion trilinear couplings A_u , A_d , and A_e ,
- the third generation sfermion mass parameters $m_{\tilde{Q}}$, $m_{\tilde{t}_R}$, $m_{\tilde{b}_R}$, $m_{\tilde{L}}$, and $m_{\tilde{\tau}_R}$,
- the third generation trilinear couplings A_t , A_b , and A_τ .

For the exact definition of these parameters and a discussion of the assumptions under which the MSSM parameter space reduces to this subset, we refer the reader to [22]. Scanning this 22-dimensional parameter space and implementing the relevant experimental bounds, in particular those from direct searches of SUSY particles at the Tevatron, is still a difficult task [73]. Fortunately the cross sections that we study in this paper turn out to be insensitive to most of the parameters above. As a result we still obtain reliable upper limits for the cross sections by scanning over an even smaller number of parameters and imposing conservative sparticle mass limits in order to satisfy the Tevatron bounds. Let us therefore take a moment to motivate our choice of independent variables for the parameter scans.

In the three-generation 2HDM we obtained the largest (scalar and pseudoscalar) Higgs production cross sections for $\tan\beta \lesssim 1$, because the $gg \rightarrow \phi$ production mechanism is enhanced in that case. In the pMSSM the bounds on the lightest Higgs-boson mass (which now depends on $\tan\beta$) require $\tan\beta \gtrsim 3$. In that case the Higgs production rate due to gluon fusion is much smaller than for $\tan\beta \sim 1$. However, for very large values of $\tan\beta$ the $\phi b\bar{b}$ couplings are enhanced and the $b\bar{b} \rightarrow \phi$ production mechanism (at the LHC) can become the dominant one. In the pMSSM the largest Higgs-boson production cross sections are obtained in this scenario. Of course the $\phi \rightarrow b\bar{b}$ partial decay widths then dominate the total width and the branching ratios for other decay modes are suppressed. Nonetheless, the largest $pp \rightarrow \phi \rightarrow VV'$ cross sections are obtained at large $\tan\beta$. In this case the production cross sections $\sigma(pp \rightarrow \phi)$ and the total decay widths Γ_ϕ are both approximately proportional to the strongly enhanced $\phi b\bar{b}$ coupling. Thus any dependence on the pMSSM parameters that enters through loop corrections to the $\phi b\bar{b}$ vertices cancels when we compute the signal cross sections $\sigma(pp \rightarrow \phi \rightarrow VV')$, because they are proportional to the ratio $\sigma(pp \rightarrow \phi)/\Gamma_\phi$.

For determining the relevant pMSSM parameters it is therefore sufficient to look at the partial widths of the $\phi \rightarrow VV'$ decay processes. As explained earlier, the only SUSY particles contributing to the $A \rightarrow VV'$ amplitudes are charginos and neutralinos. Their masses and couplings depend only on the parameters $\tan\beta$, μ , M_1 , M_2 , and m_A . The latter parameter enters through the Higgs mixing angle α . A dependence on the other parameters is introduced if loop corrections to α are taken into account. The loop corrections to α are calculated from self-energy corrections to the neutral scalar Higgs propagators. The same self-energies determine the physical mass of the light

Higgs boson, which in turn is subject to strong experimental constraints. The dominant contributions to these self-energies come from loops of top quarks and top squarks, due to the large top Yukawa coupling. We therefore expect our results to be also sensitive to those pMSSM parameters which affect the top squark masses and couplings, i.e. $m_{\tilde{Q}}$, $m_{\tilde{t}_R}$, and A_t . For the $H \rightarrow WW, ZZ$ decays the situation is even simpler: the scalar Higgs bosons couple to W and Z bosons at tree level with couplings proportional to $\cos(\beta - \alpha)$, and the dominant SUSY corrections to these vertices are obtained by replacing α by α_{eff} in the vertex factors.

These considerations motivate us to set

$$\begin{aligned} A_u = A_d = A_e = A_\tau = A_b = 0 \quad , \\ m_{\tilde{q}} = m_{\tilde{u}_R} = m_{\tilde{d}_R} = m_{\tilde{l}} = m_{\tilde{e}_R} = m_{\tilde{Q}} = m_{\tilde{b}_R} = m_{\tilde{L}} = m_{\tilde{\tau}_R} \equiv m_S \quad . \end{aligned} \quad (23)$$

Furthermore we impose the GUT relation

$$M_1 = \frac{5}{3} \tan^2 \theta_W M_2 \quad (24)$$

and use

$$\tan \beta \quad , \quad m_A \quad , \quad \mu \quad , \quad M_2 \quad , \quad M_3 \quad , \quad m_{\tilde{t}_R} \quad , \quad A_t \quad , \quad m_S \quad (25)$$

as independent variables for the parameter scans. On this reduced parameter space we apply the experimental constraints from direct Higgs-boson searches, as explained in section 3. Furthermore we require that all charginos and neutralinos are heavier than 100 GeV and 60 GeV, respectively. The light top squark is required to be heavier than 100 GeV while all other sfermions are taken to be heavier than 350 GeV. Note that bounds from fits to the oblique electroweak parameters are not applicable here, because the MSSM contains new particles which couple directly to SM fermions.

Within these constraints we obtain the following upper limits on the cross sections of the LHC reactions $pp \rightarrow A \rightarrow VV'$:

$$\begin{aligned} \sigma(pp \rightarrow A \rightarrow WW) &\lesssim 2.0 \text{ fb} \quad , & \sigma(pp \rightarrow A \rightarrow ZZ) &\lesssim 0.33 \text{ fb} \quad , \\ \sigma(pp \rightarrow A \rightarrow \gamma\gamma) &\lesssim 0.27 \text{ fb} \quad , & \sigma(pp \rightarrow A \rightarrow Z\gamma) &\lesssim 0.75 \text{ fb} \quad . \end{aligned} \quad (26)$$

As mentioned earlier in this section, the maximal values are obtained for $\tan \beta \sim 20$ and values slightly above this number. In accordance with [12] we find that the non-SUSY contributions to the $A \rightarrow VV'$ decays lead to branching ratios below 10^{-6} in this region of parameter space. However, the contributions from loops of charginos and neutralinos can increase the branching ratios to the order of 10^{-5} . The largest $A \rightarrow VV'$ partial decay widths are obtained if m_A is close to a two-chargino *and* a two-neutralino threshold, while the largest A production rates are obtained for small m_A . Therefore, parameter space regions with the largest $pp \rightarrow A \rightarrow VV'$ cross sections are characterized by

$$m_{\chi_1^\pm} \approx m_{\chi_2^0} \approx 100 \text{ GeV} \quad , \quad m_A \approx 200 \text{ GeV} \quad . \quad (27)$$

At $\tan\beta = 20$ this is realized for

$$M_2 \approx 127 \text{ GeV} \quad , \quad \mu \approx 220 \text{ GeV} \quad . \quad (28)$$

The other parameters from (25) have only a weak influence on $\sigma_{A \rightarrow VV'}$, but must of course be chosen appropriately to satisfy the experimental bounds on the pMSSM parameter space. In the subset of this space we consider here, the phenomenologically acceptable models typically contain a light top squark with $m_{\tilde{t}_1} \sim 120 \text{ GeV}$ and a heavy stop with a mass between 550 GeV and 600 GeV.

6 Top-colour assisted technicolour

An alternative to the Higgs mechanism is EWSB triggered by the condensation of (new) fermion-antifermion pairs. Phenomenologically viable scenarios of this type include models based on the concept of top-colour assisted technicolour⁸ (TC2) [74], [4, 5]. These models have two separate strongly interacting sectors in order to explain EWSB and the large top-quark mass. Technicolour interactions (TC) are responsible for most of EWSB via the condensation of techni-fermions, $\langle \bar{T}T \rangle$ ($T = U, D$), but contribute very little to the top-quark mass m_t . The top-colour interactions generate the bulk of m_t through condensation of top-quark pairs $\langle \bar{t}t \rangle$, but make only a small contribution to EWSB. The spin-zero states of TC2 are bound-states of t, b and of the techni-fermions. These two sets of bound-states form two $SU(2)_L$ doublets Φ_{TC}, Φ_t , whose couplings to the electroweak gauge bosons and to t are formally equivalent to those of a two-Higgs doublet model. The physical spin-zero states include

- a heavy neutral scalar H_{TC} with a mass of order 1 TeV,
- a neutral scalar H_t which is a $\bar{t}t$ bound state. Its mass is expected to be of the order $2m_t$ when estimated à la Nambu-Jona-Lasinio, but could in fact be lighter [75].
- a neutral “top-pion” Π^0 and a pair of charged ones, Π^\pm , whose masses are predicted to be of the order of a few hundred GeV [74, 76].

Several variants of TC2 were discussed in the literature, [4, 74]. Below we consider for definiteness TC2 with one family of technifermions.

The couplings of spin-zero states to the weak gauge bosons and to the t and b quarks can be obtained from an effective $SU(2)_L \times U(1)_Y$ invariant Lagrangian involving the doublets Φ_{TC}, Φ_t [77]. The interactions of the top quark with H_t and Π^0 are given by:

$$\mathcal{L}_{Y,t} = -\frac{Y_t}{\sqrt{2}} \bar{t}t H_t - \frac{Y_\pi}{\sqrt{2}} \bar{t}i\gamma_5 t \Pi^0 \quad , \quad (29)$$

⁸Again, to avoid misunderstandings: we consider here TC2 models with three quark-generations.

where $Y_\pi = (Y_t v_T - \varepsilon_t f_\pi)/v$ and $(Y_t f_\pi + \varepsilon_t v_T)/\sqrt{2} = m_t$. Here f_π denotes the value of the top-quark condensate which is estimated in the TC2 models to lie between $40 \text{ GeV} \lesssim f_\pi \lesssim 80 \text{ GeV}$ [74, 77]. Once f_π is fixed, v_T is determined by the EWSB requirement that $f_\pi^2 + v_T^2 = v^2 = (246 \text{ GeV})^2$. The parameter ε_t denotes the technicolour contribution to the top mass which is small by construction. The large top-quark mass thus amounts to large top Yukawa couplings Y_t, Y_π , e.g., $Y_t \approx Y_\pi \approx 3$ for $f_\pi \simeq 70 \text{ GeV}$ and small ε_t . On the other hand the couplings of H_t and Π^0 to b quarks are significantly suppressed as compared with the SM Higgs $b\bar{b}$ coupling. By construction, the top-colour interactions do not generate a direct contribution to the mass of the b quark. In TC2 models, the mass of the b quark is due to extended technicolour interactions and to top-colour instanton effects. One may use the following effective coupling of Π^0 to b quarks:

$$\mathcal{L}_{Y,b} = -\varepsilon_b \frac{f_\pi}{\sqrt{2}v} \bar{b} i \gamma_5 b \Pi^0 \quad , \quad (30)$$

where $\varepsilon_b = m_b \sqrt{2}/v_T$. With $m_b = 4.8 \text{ GeV}$ and $f_\pi \leq 80 \text{ GeV}$ one gets $\varepsilon_b \leq 0.03$.

Experimental constraints on the TC2 models were analyzed in [78–81]. The relevant constraints come from $b \rightarrow s\gamma$ decays, the LEP measurement of the hadronic $Z \rightarrow b\bar{b}$ branching ratio R_b and the oblique electroweak parameter T . The bound from $b \rightarrow s\gamma$ decays is satisfied if $\varepsilon_t \lesssim 0.1$ [80]. The bounds on the parameters of the TC2 models that result from R_b and T are considerably weaker than the corresponding ones in the 2HDM due to additional contributions from extended technicolour and topcolour gauge bosons [79, 81]. In [79] it was found that top-pion masses as low as 280 GeV are still allowed for $\varepsilon_t = 0.1$ and $f_\pi = 70 \text{ GeV}$. In order to estimate the maximal values of the LHC Π^0 and H_t production cross sections⁹, we have therefore chosen these parameter values.

The main partonic production reaction of the neutral top-pion and of H_t is gluon fusion. In many TC2 models [4, 74], technifermions do not have QCD charges and do therefore not contribute to this reaction. The amplitudes $gg \rightarrow \Pi^0, H_t$ are then dominated by top-quark loops [74, 83–85]. As to $gg \rightarrow H_t$, the contribution of topcolour gauge bosons is negligible [85].

On the other hand, technifermions do contribute to the decays of the top-pion Π^0 into $\gamma\gamma, Z\gamma, ZZ$. The technicolour component of the mass eigenstate Π^0 , which is part of a $SU(2)_L$ triplet, has effective couplings to weak gauge bosons through the chiral anomaly. These “anomalous” terms depend on the specific technifermion sector of TC2, and can be determined by the respective chiral anomaly of the associated currents [86, 87]. Here we consider for definiteness one family of technifermions. The respective anomalous contributions to $\Pi^0 \rightarrow \gamma\gamma, Z\gamma, ZZ$ are readily computed; they can be found, for instance, in [87, 88]. (Notice that the anomaly factor for $\Pi^0 \rightarrow W^+W^-$ is zero.)

⁹In [82] the hadronic production of light techni-pions and their decays, in particular to two photons, were investigated within several technicolour models.

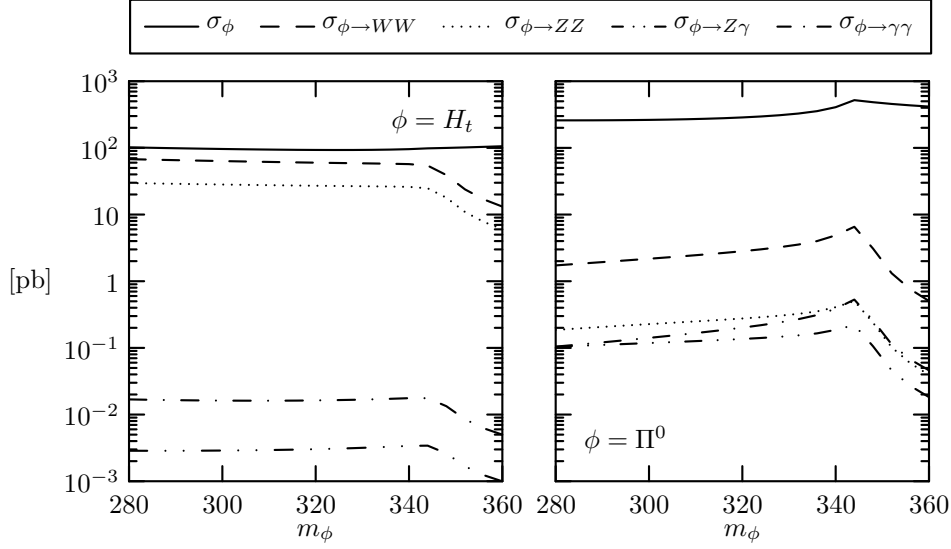


Figure 3: The LHC cross sections $\sigma(pp \rightarrow \phi)$ and $\sigma(pp \rightarrow \phi \rightarrow VV')$ as functions of m_ϕ (with $\phi \in \{H_t, \Pi^0\}$ and $VV' \in \{WW, ZZ, \gamma\gamma, Z\gamma\}$) in TC2 with $\varepsilon_t = 0.1$ and $f_\pi = 70$ GeV.

Figure 3 shows the LHC production cross sections for H_t , Π^0 and the cross section times branching ratios for the WW , ZZ , $\gamma\gamma$ and $Z\gamma$ final states as functions of the mass of the respective resonance for the parameters given above. We see that the H_t and Π^0 production rates are quite large with values of 100 pb and 200 to 500 pb, respectively. If m_{H_t} is below the $t\bar{t}$ threshold, the H_t decays dominantly into WW and ZZ for the above parameter values, and we obtain cross sections $\sigma(pp \rightarrow H_t \rightarrow WW, ZZ)$ of about 60 pb and 25 pb, respectively. The loop-mediated decays into $\gamma\gamma$ and $Z\gamma$ have only very small branching ratios. The top-pion Π^0 decays dominantly into gluon pairs if $\Pi^0 \rightarrow t\bar{t}$ is kinematically forbidden. The cross sections become maximal if the mass of the decaying particle is just below the $t\bar{t}$ threshold. For $m_{\Pi^0} = m_{H_t} = 340$ GeV we have

$$\begin{aligned}
\sigma(pp \rightarrow \Pi^0 \rightarrow WW) &= 4.9 \text{ pb} \quad , & \sigma(pp \rightarrow H_t \rightarrow WW) &= 57 \text{ pb} \quad , \\
\sigma(pp \rightarrow \Pi^0 \rightarrow ZZ) &= 0.41 \text{ pb} \quad , & \sigma(pp \rightarrow H_t \rightarrow ZZ) &= 26 \text{ pb} \quad , \\
\sigma(pp \rightarrow \Pi^0 \rightarrow \gamma\gamma) &= 0.39 \text{ pb} \quad , & \sigma(pp \rightarrow H_t \rightarrow \gamma\gamma) &= 0.02 \text{ pb} \quad , \\
\sigma(pp \rightarrow \Pi^0 \rightarrow Z\gamma) &= 0.19 \text{ pb} \quad , & \sigma(pp \rightarrow H_t \rightarrow Z\gamma) &= 0.003 \text{ pb} \quad .
\end{aligned} \tag{31}$$

Without the anomalous contributions $\sigma_{\Pi^0 \rightarrow \gamma\gamma}$ would be larger by a factor ~ 2.5 , while $\sigma_{\Pi^0 \rightarrow ZZ}$ would decrease by about a factor ~ 2 . The cross section $\sigma_{\Pi^0 \rightarrow Z\gamma}$ remains essentially unchanged.

It is worth emphasizing that the cross sections for $\Pi^0 \rightarrow \gamma\gamma, Z\gamma$ are much larger than the corresponding ones for H_t . As to the possible size of the ratio $\sigma_{\Pi^0 \rightarrow VV}/\sigma_{H_t \rightarrow VV}$ ($V = W, Z$) the values in (31) are, for the specific technifermion sector, rather conservative. This ratio increases for smaller values of f_π .

If Π^0 or H_t are heavier than $2m_t$ they decay dominantly into $t\bar{t}$ pairs and the branching ratios of the other decay modes become very small.

7 Summary and Conclusions

We have computed and analyzed the LHC cross sections for the production of a heavy pseudoscalar Higgs boson A , and also those of a heavy scalar H , and their subsequent decays into electroweak gauge bosons in several SM extensions. We determined and scanned the phenomenologically allowed regions of the corresponding parameter spaces in order to find the largest possible values of these cross sections. Within the non-SUSY models analyzed here we considered spin-zero states A, H with masses $m_{A,H} \lesssim 2m_t$, for reasons stated in Section 2.

For models with elementary Higgs fields, the largest cross sections $\sigma_{A \rightarrow VV'}$ for A were found in the decoupling limit of a 2HDM with a fourth generation of chiral fermions and $\tan\beta \approx 6.3$. The total LHC production rate for A can become of the order of 800 pb in this scenario, without violating bounds from direct Higgs-boson searches at the Tevatron. The signal cross sections for the decays of A into electroweak gauge bosons can then be of the order of a few picobarn.

In the 3-generation type-II 2HDM we found the largest cross sections $\sigma_{A \rightarrow VV'}$ in the decoupling limit with $\tan\beta \approx 0.75$. For the WW and $\gamma\gamma$ final states the maximum values are of the order of 0.1 pb. For the ZZ and $Z\gamma$ final states they are smaller by about one order of magnitude. Extending the 2HDM by vector-like quarks in the way as was done in [69] does not change the maximum allowed values of the cross sections significantly.

In the MSSM we obtained the largest pseudoscalar cross sections for large $\tan\beta$ and for a spectrum where m_A is close to both a two-chargino and a two-neutralino threshold. Loops of charginos and neutralinos then yield the dominant contributions to the $A \rightarrow VV'$ decay rates. However, the resulting signal cross sections are at most a few femtobarn.

Finally we studied topcolour-assisted technicolour as a paradigm for models with composite spin-zero states. Though conceptually very different, the “Higgs sector” of this model and the couplings of the spin-zero particles to top quarks and electroweak gauge bosons corresponds to a 2HDM with small $\tan\beta$. Experimental constraints on the parameter space of these models from measurements of R_b and the ρ parameter are relaxed due to contributions from technicolour and topcolour gauge bosons. In a TC2 model with one family of technifermions, the maximal allowed signal cross sections for decays of the pseudoscalar top-pion Π^0 into electroweak gauge bosons are of the order of 5 pb for $\Pi^0 \rightarrow WW$ and between 0.1 pb and 0.5 pb for $\Pi^0 \rightarrow Z\gamma, \gamma\gamma, ZZ$. The amplitude of the strongest decay mode, $\Pi^0 \rightarrow WW$, is actually insensitive to the specific technifermion sector.

In conclusion we found that, with the exception of the MSSM, all the models analyzed above permit the cross sections for $pp \rightarrow A \rightarrow VV'$ to be of observable size at the LHC, in particular for $A \rightarrow WW, \gamma\gamma$. The cross sections $\sigma_{A \rightarrow \gamma\gamma}$ and $\sigma_{A \rightarrow Z\gamma}$ are typically

one to two orders of magnitude larger than the corresponding ones for a heavy scalar H . Moreover, it is also possible that $\sigma_{A \rightarrow WW}$ is of the same order of magnitude as $\sigma_{H \rightarrow WW}$, as Figs. 1 and 2 show. Obviously this does not mean that these are the most probable channels for discovering A . Very likely, the discovery modes would be $A \rightarrow b\bar{b}$, $\tau^+\tau^-$, Zh , or $A \rightarrow t\bar{t}$, depending on the mass spectra and coupling strengths. But a pseudoscalar resonance would then be observable at the LHC also in its decays into electroweak gauge bosons, in particular in WW and $\gamma\gamma$ final states.

Acknowledgments

We would like to thank Alexander Belyaev, Jens Erler, Ulrich Haisch, Jürgen Rohrwild, Oscar Stål, and Peter Zerwas for fruitful discussions and information about their work. A special thanks goes to Karina Williams for patiently answering questions about FeynHiggs and HiggsBounds.

This work was supported by Deutsche Forschungsgemeinschaft DFG SFB/TR9 and BMBF. P.G. is supported by a stipend from the DFG funded RWTH Graduiertenkolleg “Elementarteilchenphysik an der TeV Skala”.

References

- [1] A. Djouadi, *Phys. Rept.* **457** (2008) 1–216, [arXiv:hep-ph/0503172](#).
- [2] A. Djouadi, *Phys. Rept.* **459** (2008) 1–241, [arXiv:hep-ph/0503173](#).
- [3] E. Accomando *et al.*, [arXiv:hep-ph/0608079](#).
- [4] C. T. Hill and E. H. Simmons, *Phys. Rept.* **381** (2003) 235–402, [arXiv:hep-ph/0203079](#).
- [5] G. Cvetič, *Rev. Mod. Phys.* **71** (1999) 513–574, [arXiv:hep-ph/9702381](#).
- [6] D. E. Morrissey, T. Plehn, and T. M. P. Tait, [arXiv:0912.3259 \[hep-ph\]](#).
- [7] A. Bredenstein, A. Denner, S. Dittmaier, and M. M. Weber, *JHEP* **02** (2007) 080, [arXiv:hep-ph/0611234](#).
- [8] **CDF and D0** Collaboration, T. Aaltonen *et al.*, *Phys. Rev. Lett.* **104** (2010) 061804.
- [9] S. Asai *et al.*, *Eur. Phys. J.* **C32S2** (2004) 19–54, [arXiv:hep-ph/0402254](#).
- [10] S. Abdullin *et al.*, *Eur. Phys. J.* **C39S2** (2005) 41–61.
- [11] A. Mendez and A. Pomarol, *Phys. Lett.* **B272** (1991) 313–318.

- [12] J. F. Gunion, H. E. Haber, and C. Kao, *Phys. Rev.* **D46** (1992) 2907–2917.
- [13] C. A. Nelson, *Phys. Rev.* **D37** (1988) 1220.
- [14] A. Soni and R. M. Xu, *Phys. Rev.* **D48** (1993) 5259–5263, [arXiv:hep-ph/9301225](#).
- [15] A. Skjold and P. Osland, *Phys. Lett.* **B311** (1993) 261–265, [arXiv:hep-ph/9303294](#).
- [16] V. D. Barger, K.-m. Cheung, A. Djouadi, B. A. Kniehl, and P. M. Zerwas, *Phys. Rev.* **D49** (1994) 79–90, [arXiv:hep-ph/9306270](#).
- [17] T. Arens and L. M. Sehgal, *Z. Phys.* **C66** (1995) 89–94, [arXiv:hep-ph/9409396](#).
- [18] S. Y. Choi, D. J. Miller, M. M. Muhlleitner, and P. M. Zerwas, *Phys. Lett.* **B553** (2003) 61–71, [arXiv:hep-ph/0210077](#).
- [19] C. P. Buszello, I. Fleck, P. Marquard, and J. J. van der Bij, *Eur. Phys. J.* **C32** (2004) 209–219, [arXiv:hep-ph/0212396](#).
- [20] R. M. Godbole, D. J. Miller, and M. M. Muhlleitner, *JHEP* **12** (2007) 031, [arXiv:0708.0458 \[hep-ph\]](#).
- [21] A. De Rujula, J. Lykken, M. Pierini, C. Rogan, and M. Spiropulu, [arXiv:1001.5300 \[hep-ph\]](#).
- [22] A. Djouadi, J.-L. Kneur, and G. Moultaka, *Comput. Phys. Commun.* **176** (2007) 426–455, [arXiv:hep-ph/0211331](#).
- [23] T. Hahn, S. Heinemeyer, F. Maltoni, G. Weiglein, and S. Willenbrock, [arXiv:hep-ph/0607308](#).
- [24] R. M. Barnett, H. E. Haber, and D. E. Soper, *Nucl. Phys.* **B306** (1988) 697.
- [25] D. A. Dicus and S. Willenbrock, *Phys. Rev.* **D39** (1989) 751.
- [26] S. Dittmaier, M. Kramer, and M. Spira, *Phys. Rev.* **D70** (2004) 074010, [arXiv:hep-ph/0309204](#).
- [27] S. Heinemeyer, W. Hollik, and G. Weiglein, *Comput. Phys. Commun.* **124** (2000) 76–89, [arXiv:hep-ph/9812320](#).
- [28] R. Harlander, *J. Phys.* **G35** (2008) 033001.
- [29] S. Catani, D. de Florian, M. Grazzini, and P. Nason, *JHEP* **07** (2003) 028, [arXiv:hep-ph/0306211](#). The tables interpolated by FeynHiggs were taken from F. Maltoni, <http://maltoni.home.cern.ch/maltoni/TeV4LHC/index.html>.

- [30] P. Bechtle, O. Brein, S. Heinemeyer, G. Weiglein, and K. E. Williams, *Comput. Phys. Commun.* **181** (2010) 138–167, [arXiv:0811.4169 \[hep-ph\]](#).
- [31] M. E. Peskin and T. Takeuchi, *Phys. Rev. Lett.* **65** (1990) 964–967.
- [32] G. Altarelli and R. Barbieri, *Phys. Lett.* **B253** (1991) 161–167.
- [33] O. Brein, *Comput. Phys. Commun.* **170** (2005) 42–48, [arXiv:hep-ph/0407340](#).
- [34] T. Hahn, *Comput. Phys. Commun.* **140** (2001) 418–431, [arXiv:hep-ph/0012260](#).
- [35] T. Hahn and C. Schappacher, *Comput. Phys. Commun.* **143** (2002) 54–68, [arXiv:hep-ph/0105349](#).
- [36] T. Hahn and M. Perez-Victoria, *Comput. Phys. Commun.* **118** (1999) 153–165, [arXiv:hep-ph/9807565](#).
- [37] T. Hahn and M. Rauch, *Nucl. Phys. Proc. Suppl.* **157** (2006) 236–240, [arXiv:hep-ph/0601248](#).
- [38] J. F. Gunion, H. E. Haber, G. L. Kane, and S. Dawson, *The Higgs Hunter’s Guide*. Perseus Publishing, Cambridge, Mass., 2000.
- [39] J. F. Gunion and H. E. Haber, *Phys. Rev.* **D67** (2003) 075019, [arXiv:hep-ph/0207010](#).
- [40] A. K. Grant, *Phys. Rev.* **D51** (1995) 207–217, [arXiv:hep-ph/9410267](#).
- [41] H. E. Haber and H. E. Logan, *Phys. Rev.* **D62** (2000) 015011, [arXiv:hep-ph/9909335](#).
- [42] K. Cheung and O. C. W. Kong, *Phys. Rev.* **D68** (2003) 053003, [arXiv:hep-ph/0302111](#).
- [43] W. Grimus, L. Lavoura, O. M. Ogreid, and P. Osland, *J. Phys.* **G35** (2008) 075001, [arXiv:0711.4022 \[hep-ph\]](#).
- [44] A. Wahab El Kaffas, P. Osland, and O. M. Ogreid, *Phys. Rev.* **D76** (2007) 095001, [arXiv:0706.2997 \[hep-ph\]](#).
- [45] I. F. Ginzburg and I. P. Ivanov, *Phys. Rev.* **D72** (2005) 115010, [arXiv:hep-ph/0508020](#).
- [46] C. Amsler *et al.*, *Phys. Lett.* **B667** (2008) 1.
- [47] W. Grimus, L. Lavoura, O. M. Ogreid, and P. Osland, *Nucl. Phys.* **B801** (2008) 81–96, [arXiv:0802.4353 \[hep-ph\]](#).

- [48] C. D. Froggatt, R. G. Moorhouse, and I. G. Knowles,
Phys. Rev. **D45** (1992) 2471–2481.
- [49] D. Eriksson, J. Rathsmann, and O. Stal,
Comput. Phys. Commun. **181** (2010) 189–205, [arXiv:0902.0851 \[hep-ph\]](#).
- [50] J. Erler, [arXiv:1002.1320 \[hep-ph\]](#).
- [51] J. Erler and P. Langacker, [arXiv:1003.3211 \[hep-ph\]](#).
- [52] M. Maniatis, A. von Manteuffel, and O. Nachtmann,
Eur. Phys. J. **C57** (2008) 739–762, [arXiv:0711.3760 \[hep-ph\]](#).
- [53] M. Maniatis and O. Nachtmann, *JHEP* **05** (2009) 028,
[arXiv:0901.4341 \[hep-ph\]](#).
- [54] G. D. Kribs, T. Plehn, M. Spannowsky, and T. M. P. Tait,
Phys. Rev. **D76** (2007) 075016, [arXiv:0706.3718 \[hep-ph\]](#).
- [55] B. Holdom *et al.*, *PMC Phys.* **A3** (2009) 4, [arXiv:0904.4698 \[hep-ph\]](#).
- [56] M. Hashimoto, [arXiv:1001.4335 \[hep-ph\]](#).
- [57] J. Alwall *et al.*, *Eur. Phys. J.* **C49** (2007) 791–801, [arXiv:hep-ph/0607115](#).
- [58] M. Bobrowski, A. Lenz, J. Riedl, and J. Rohrwild,
Phys. Rev. **D79** (2009) 113006, [arXiv:0902.4883 \[hep-ph\]](#).
- [59] **CDF** Collaboration, D. Cox, [arXiv:0910.3279 \[hep-ex\]](#).
- [60] **CDF** Collaboration, T. Aaltonen *et al.*, [arXiv:0912.1057 \[hep-ex\]](#).
- [61] S. Berge, W. Bernreuther, and J. Ziethe, *Phys. Rev. Lett.* **100** (2008) 171605,
[arXiv:0801.2297 \[hep-ph\]](#).
- [62] S. Berge and W. Bernreuther, *Phys. Lett.* **B671** (2009) 470–476,
[arXiv:0812.1910 \[hep-ph\]](#).
- [63] P. H. Frampton, P. Q. Hung, and M. Sher, *Phys. Rept.* **330** (2000) 263,
[arXiv:hep-ph/9903387](#).
- [64] F. del Aguila, M. Perez-Victoria, and J. Santiago, *JHEP* **09** (2000) 011,
[arXiv:hep-ph/0007316](#).
- [65] F. del Aguila, M. Perez-Victoria, and J. Santiago,
Phys. Lett. **B492** (2000) 98–106, [arXiv:hep-ph/0007160](#).
- [66] J. A. Aguilar-Saavedra, *JHEP* **11** (2009) 030, [arXiv:0907.3155 \[hep-ph\]](#).

- [67] T. Appelquist, H.-C. Cheng, and B. A. Dobrescu, *Phys. Rev.* **D64** (2001) 035002, [arXiv:hep-ph/0012100](#).
- [68] N. Arkani-Hamed, A. G. Cohen, E. Katz, and A. E. Nelson, *JHEP* **07** (2002) 034, [arXiv:hep-ph/0206021](#).
- [69] W. Bernreuther, P. Gonzalez, and M. Wiebusch, [arXiv:0909.3772 \[hep-ph\]](#).
- [70] M. Frank *et al.*, *JHEP* **02** (2007) 047, [arXiv:hep-ph/0611326](#).
- [71] G. Degrassi, S. Heinemeyer, W. Hollik, P. Slavich, and G. Weiglein, *Eur. Phys. J.* **C28** (2003) 133–143, [arXiv:hep-ph/0212020](#).
- [72] S. Heinemeyer, W. Hollik, and G. Weiglein, *Eur. Phys. J.* **C9** (1999) 343–366, [arXiv:hep-ph/9812472](#).
- [73] C. F. Berger, J. S. Gainer, J. L. Hewett, and T. G. Rizzo, *JHEP* **02** (2009) 023, [arXiv:0812.0980 \[hep-ph\]](#).
- [74] C. T. Hill, *Phys. Lett.* **B345** (1995) 483–489, [arXiv:hep-ph/9411426](#).
- [75] R. S. Chivukula, B. A. Dobrescu, H. Georgi, and C. T. Hill, *Phys. Rev.* **D59** (1999) 075003, [arXiv:hep-ph/9809470](#).
- [76] G. Buchalla, G. Burdman, C. T. Hill, and D. Kominis, *Phys. Rev.* **D53** (1996) 5185–5200, [arXiv:hep-ph/9510376](#).
- [77] A. K. Leibovich and D. L. Rainwater, *Phys. Rev.* **D65** (2002) 055012, [arXiv:hep-ph/0110218](#).
- [78] G. Burdman and D. Kominis, *Phys. Lett.* **B403** (1997) 101–107, [arXiv:hep-ph/9702265](#).
- [79] C.-X. Yue, Y.-P. Kuang, X.-L. Wang, and W.-b. Li, *Phys. Rev.* **D62** (2000) 055005, [arXiv:hep-ph/0001133](#).
- [80] B. Balaji, *Phys. Rev.* **D53** (1996) 1699–1702, [arXiv:hep-ph/9505313](#).
- [81] G.-H. Wu, *Phys. Rev. Lett.* **74** (1995) 4137–4140, [arXiv:hep-ph/9412206](#).
- [82] A. Belyaev, A. Blum, R. S. Chivukula, and E. H. Simmons, *Phys. Rev.* **D72** (2005) 055022, [arXiv:hep-ph/0506086](#).
- [83] G. Burdman, *Phys. Rev. Lett.* **83** (1999) 2888–2891, [arXiv:hep-ph/9905347](#).
- [84] J.-j. Cao, Z.-h. Xiong, and J. M. Yang, *Phys. Rev.* **D67** (2003) 071701, [arXiv:hep-ph/0212114](#).
- [85] M. Hashimoto, *Phys. Rev.* **D66** (2002) 095015, [arXiv:hep-ph/0201110](#).

- [86] S. Dimopoulos, S. Raby, and G. L. Kane, *Nucl. Phys.* **B182** (1981) 77.
- [87] J. R. Ellis, M. K. Gaillard, D. V. Nanopoulos, and P. Sikivie, *Nucl. Phys.* **B182** (1981) 529–545.
- [88] R. S. Chivukula, R. Rosenfeld, E. H. Simmons, and J. Terning, [arXiv:hep-ph/9503202](https://arxiv.org/abs/hep-ph/9503202).